

# Power Flow Analysis and Critical Design Issues of Retrofit Light-Emitting Diode (LED)

## Light Bulb

Sinan Li, Huanting Chen, Siew-Chong Tan, *Senior Member, IEEE*, S.Y.R. Hui, *Fellow, IEEE*

Department of Electrical & Electronic Engineering  
The University of Hong Kong  
Hong Kong, China

Eberhard Waffenschmidt, *Senior Member, IEEE*

Faculty of Information, Media, and Electrical Engineering Cologne University of Applied Science  
Cologne, Germany

**Abstract**—For retrofit applications, some high-brightness (HB) light-emitting diode (LED) products have the same form factor restrictions as existing incandescent light bulbs. Such form factor constraints may restrict the design and optimal performance of the LED technology. In this paper, some critical design issues for a commercial LED bulb designed for replacing an E27 incandescent lamp are quantitatively analyzed. The analysis involves a power audit on such densely packed LED system so that the amounts of power consumption in (1) the LED driver, (2) the LED wafer, (3) the phosphor coating, and (4) the bulb translucent cover are quantified. The outcomes of such an audit enable R&D engineers to identify the critical areas that need further improvements in a compact LED bulb design. The strong dependence of the luminous output of the compact LED bulb on ambient temperature is also highlighted.

## I. INTRODUCTION

Light-emitting diodes (LED) have emerged as an important technology on a growing list of applications. This is mainly due to their preponderant long lifetime, environmentally friendly characteristic, high luminous efficacy, and having the ability to illuminate in various colors [1]–[3]. For general lighting applications, the high-brightness LEDs (HB-LEDs) are expected to replace traditional light sources such as the incandescent and fluorescent lamps [4]. However, it may still take some time before the HB-LEDs can really dominate the general lighting market because of the many complicated problems that involve the photometric, electrical, thermal, and reliability related issues of the LED system [3], [5]–[8]. This paper is an extended version of a conference paper [14]. In this paper, we investigate a classic example of a white LED light bulb for replacing an E27 incandescent lamp such that future challenges in optimizing such compact LED systems could be systematically tackled. The critical design issues of a compact LED bulb are identified and addressed.

An HB-LED system for general illumination usually comprises several functional stages:

- LED ballast—It supplies electric power to the LED chips from the power source;
- LED chips—They receive electric power from the ballast and radiate white light;
- Lamp cover or lenses—It scatters the emitted light as a way to satisfy certain color temperature or viewing angle requirements. The optical power emitted from the LED chips are partially lost in this stage;
- Heatsink—It dissipates the heat generated from the ballast and the LEDs and all other heat sources.

## II. ENERGY FLOW CHART AND POWER AUDIT OF THE LED SYSTEM

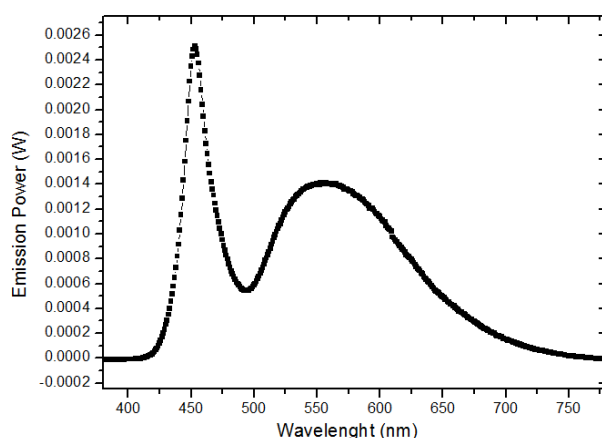


Fig. 1. Light spectrum of a phosphor-based white LED.

This study focuses on a power audit of an LED bulb based on the use of phosphor-coated (PC) white LED devices. The light spectrum shown in Fig. 1 indicates that it consists of the sum of two spectra, namely one strong blue light spectrum generated directly from a GaN or InGaN LED at the 450 nm, and a second light spectrum of Stokes-shifted wavelengths emitted from the phosphor coating. During the Stokes-shift process where the phosphor absorbs the blue photon energy and emits light of longer wavelengths, there is a loss of heat energy, commonly known as the Stoke-shift loss. A detailed view of the interior structure is shown in Fig. 2.

For simplicity, the phosphor-based LEDs can be perceived as having two power processing sub-stages: one being the blue LED chip generating blue light from electrons and the other being the phosphor layer performing the Stock-shift process. Since the phosphor-coated LED is still the most popular method of generating white light from LEDs, due to their simple manufacturing and design process for the LED system, the following analysis will be based on the phosphor-coated LED structures.

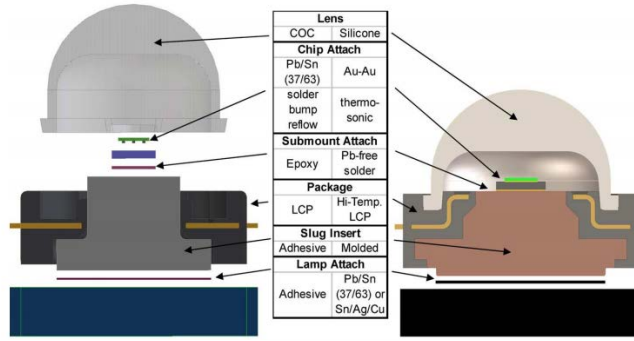


Fig. 2. A detailed inside view of the function stages of an LED package.

Based on Fig. 2, the energy flow chart can be drawn as shown in Fig. 3, which consists of five stages of energy conversion. Fig. 4 shows the photograph of the exterior and interior functional stages of the LED bulb.

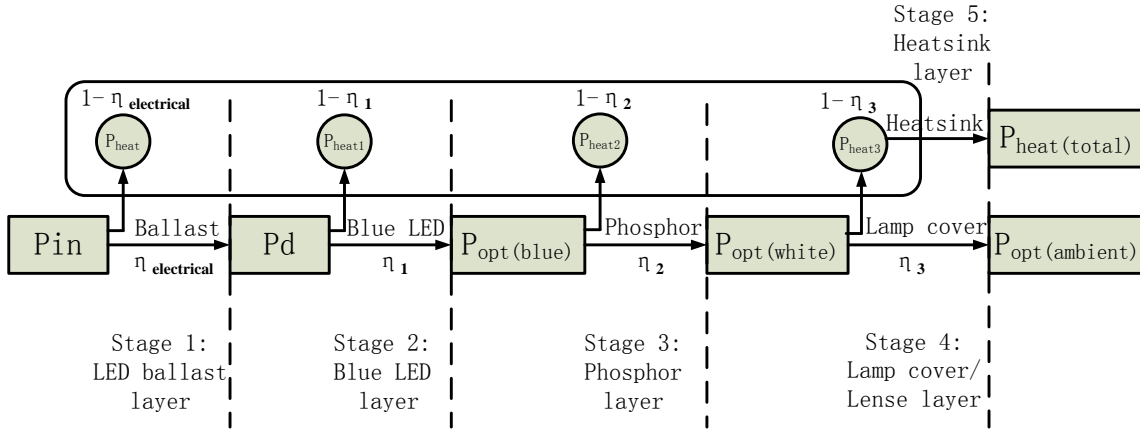


Fig. 3. Energy flow chart with the five functional stages of the LED system.

In Stage 1, the input power  $P_{in}$  is processed by the LED ballast with an efficiency of  $\eta_{\text{electrical}}$ . For linear or passive types of ballasts, the power loss is mainly due to the conduction loss of the lossy components such as the current limiting resistors, transistors and transformers, while in switched-mode ballasts, the power loss is mainly caused by switching losses, conduction loss, and core losses of magnetic components. Linear/passive ballasts are generally simpler in structure, but larger in size when compared with the switched-mode ballasts. Regardless of the type of ballasts used, the power delivered to the LED chips from the ballast can be generalized as

$$P_d = P_{in} \eta_{\text{electrical}} \quad (1)$$

where  $P_d$  is the input power of the second stage.

In Stage 2, the blue LED chips convert electric energy into light energy by emitting blue light with an efficiency of  $\eta_1$ . The emitted optical power of the blue LED,  $P_{\text{opt(blue)}}$ , is given as

$$P_{\text{opt(blue)}} = P_d \eta_1 \quad (2)$$

while the rest of the input power are converted into heat. The heat generation is related to several power-loss mechanisms, such as the leakage current power loss due to tunneling of electrons to the states of InGaN/GaN interfaces, power loss due to the effect of auger recombination, and power loss due to non-radiative recombination. Additionally, any photons generated by radiative recombination inside the LED chip may be emitted as external light or are trapped within the LED chip (caused by total internal reflection phenomenon of the semiconductor crystal), where they are finally absorbed and converted into heat. Taking all power losses into consideration, the total fraction of photons with respect to a known power level input that are emitted by the LED is known as the extraction efficiency  $\eta_1$ . Currently, the extraction efficiency of HB-LED is around 20-40% [9], which is relatively much lower than other functional stages of energy conversion, and it is therefore the most influencing factor affecting the overall efficiency of the LED lamps.

In Stage 3, the blue light carrying a power of  $P_{\text{opt(blue)}}$  is converted into white light by the phosphor with a conversion power efficiency of  $\eta_2$ . The conversion power loss is related to the quantum efficiency and absorption characteristic of the phosphor materials, and is influenced by the trapping and absorption of the photons' energy, which is eventually converted into heat by the phosphor material of the phosphor-coated (PC) LED. Currently, many commercially available phosphor materials are of good performance with a conversion efficiency  $\eta_2$  of usually higher than 90%. The optical power of the emitted white light,  $P_{\text{opt(white)}}$ , is given by

$$P_{\text{opt(white)}} = P_{\text{opt(blue)}} \eta_2 \quad (3)$$

Finally, the power of white light emitted from the phosphor coated (PC) LED will pass through Stage 4, which is the lamp cover or lenses (blue LED coated with phosphor epoxy is also a form of lenses), where the white light will be scattered to the ambient. For this stage, the lamp covers or lenses act as light filters, which in the process of scattering the light, partially trap photons within the covers/lenses converting them into extra heat, thereby incurring an additional form of optical power loss. Thus, the final optical output power of the light emitted to the ambient in terms of the lenses efficiency  $\eta_3$ , can be expressed as

$$P_{\text{opt(ambient)}} = P_{\text{opt(white)}} \eta_3 \quad (4)$$

In order to analyze the power flow of each functional stage, their energy conversion efficiencies  $\eta$  must be individually evaluated and compared. Practically, it is much easier to measure the optical power emitted from the respective stages than to measure the heat power dissipated from the stages. Hence, in the following discussion, the optical power coefficient  $k_{\text{opt}}$  is defined for each stage, which is the ratio of optical power  $P_{\text{opt}}$  over the total input power to LED  $P_d$ . In the same manner, the heat dissipation coefficient  $k_h$  is defined as the ratio of heat power  $P_{\text{heat}}$  (the power that finally ends up as heat in each stage) over  $P_d$ .

$$k_{\text{opt}} = P_{\text{opt}} / P_d \quad (5)$$

$$k_h = P_{\text{heat}} / P_d \quad (6)$$

The coefficients  $k_{\text{opt}}$  and  $k_h$  can be used to derive the conversion efficiency  $\eta$  for each stage. For example, after Stage 2, the output optical power and heat power are,

$$P_{\text{opt(blue)}} = P_d k_{\text{opt1}} = P_d \eta_1 \quad (7)$$

$$P_{\text{heat1}} = P_d k_{h1} = P_d - P_{\text{opt(blue)}} = P_d (1 - \eta_1) \quad (8)$$

Therefore,

$$k_{\text{opt1}} = \eta_1 \quad (9)$$

$$k_{h1} = 1 - \eta_1 \quad (10)$$

Using (9), the conversion efficiency  $\eta_1$  can be calculated as,

$$\eta_1 = k_{opt1} = 1 - k_{h1} \quad (11)$$

Following the same approach, the relationships between  $k_{opt}$ ,  $k_h$  and  $\eta$  for each stage can be derived and are tabulated in Table I.

TABLE I. RELASHIONSHIPS BETWEEN  $k_{opt}$ ,  $k_h$  AND CONVERSION EFFICIENCIES  $\eta_1, \eta_2, \eta_3$

Energy Flow Stage	$k_{opt}$	$k_h$	$H$
2	$k_{opt1} = \eta_1$	$k_{h1} = 1 - \eta_2$	$k_{opt1}$
3	$k_{opt2} = \eta_1 \eta_2$	$k_{h2} = 1 - \eta_1 \eta_2$	$k_{opt2} / k_{opt1}$
4	$k_{opt3} = \eta_1 \eta_2 \eta_3$	$k_{h3} = 1 - \eta_1 \eta_2 \eta_3$	$k_{opt3} / k_{opt2}$

It is evident from Table I that the higher the conversion efficiency  $\eta$  in each power conversion stage, the higher the  $k_{opt}$  and the lower the  $k_h$ . From Table I, the conversion efficiency  $\eta$  of each stage can easily be derived given  $k_{opt1}$ ,  $k_{opt2}$ ,  $k_{opt3}$ . Detailed results are included and compared in Section III.

### III. EXPERIMENTAL RESULTS OF AUDITING THE POWER OF AN LED BULB

The LED system used in the experimental evaluation is a commercial warm-white LED bulb with a rated power of 8 W. It has an internal LED ballast and the bulb is comprised of all the five function stages as mentioned above. Fig. 4 illustrates some pictures of the exterior and internal functional stages of the LED bulb used in this experiment. In order to analyze the efficiency of Stokes-shift effect of converting blue light of Stage 2 (Fig.4 b) to white light of Stage 3 (Fig.4 c), the phosphor epoxy layer should be removed leaving only the blue LED wafer. However the epoxy encapsulation process is

irreversible and the layer cannot be easily removed, since the bonding wires inside the LED chips are easily broken.

In this experiment, an identical blue LED with the same characteristics (in terms of thermal, electrical and optical performance) is used to substitute the one used in the white LED bulb, as shown in Fig. 4(b). For the power audit, the experiments are conducted at the ambient temperature of 22 °C under free convection.



(a) Ballast



(b) Blue LED



(c) PC LED



(d) Heatsink



(e) Cover/Lenses



(f) LED bulb

Fig. 4. Photographs of the exterior and interior functional stages of an LED bulb.



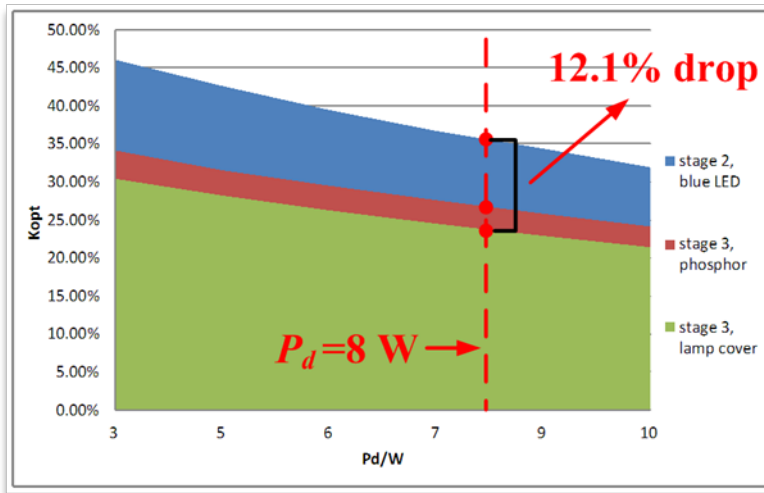


Fig. 5. Power audit of the LED bulb for the respective stages at 3 W to 10 W.

Fig. 5 shows the measurement results of the power audit of the LED bulb for each stage and at different power level  $P_d$ . The power distribution is represented by the optical efficiency  $k_{opt}$  in each stage using different colors. A thinner layer of the area between any two adjacent stages signifies a lower conversion loss between these stages, i.e., higher efficiency during conversion.

Fig. 5 gives a clear view of the energy distribution for each functional stage. For example, in Stage 2, when  $P_d = 7.22$  W (with LED conducting current of  $I_{LED} = 0.58$  A), the output optical power of blue LED is 2.65 W (with  $k_{opt1} = 36.7\%$ ). After the phosphor conversion stage, i.e., Stage 3, some power is lost and the total optical power emitted in the form of white light drops to 1.99 W (with  $k_{opt2} = 27.6\%$ ). Moreover, after the lamp cover is mounted, the actual emitted optical power left is only 1.77 W ( $k_{opt3} = 24.5\%$ ). If the output optical power is assumed to be proportional to the emitted lumen flux, we can then predict that the huge drop from  $k_{opt1}$  to  $k_{opt3}$  (12.2%) results in the same amount of reduction in the output light intensity. Finally, by taking into consideration the power loss from the LED ballast, and assuming an efficiency of  $\eta_{electrical} = 85\%$ , the final energy efficiency in this LED system will be 20.8%. This result shows that around 21% of total input electric energy has been converted as light.

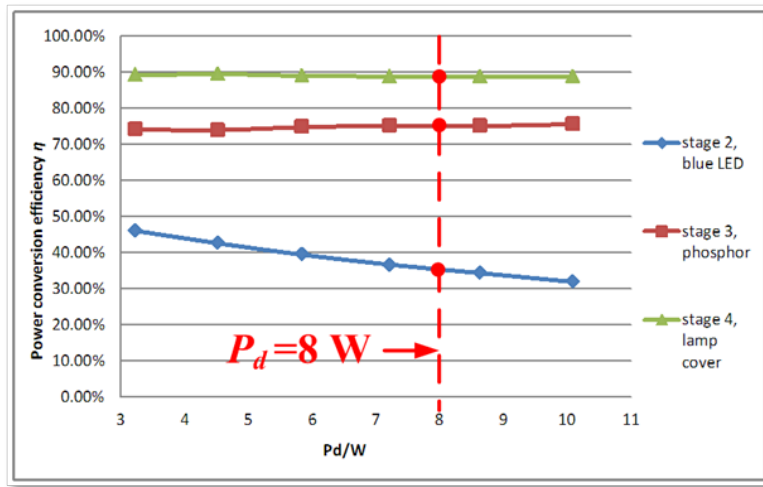


Fig. 6. Conversion efficiency of the LED bulb for Stage 2 to Stage 4 at 3 W to 10 W.

Next, the performance of the respective stages is compared using the conversion efficiency  $\eta$ . According to Table I, the efficiency of each stage is shown in Fig. 6. It can be seen that the blue LED (in Stage 2) is the most inefficient power stage among the three stages. At the low input power level of  $P_d = 3.3$  W, the blue LED converts less than 46% of  $P_d$  into optical power. As  $P_d$  increases and junction temperature goes higher, the Stage 2 conversion efficiency drops further, with merely 32% of the total energy being converted into optical power when  $P_d = 10.1$  W. Despite the low conversion efficiency of Stage 2, it should be highlighted that a blue LED efficiency of 32% is still significantly higher than that of the incandescent sources, and is comparable to the plasma discharge conversions efficiency in compact fluorescent lamps [8], [9], also shown in Fig. 7.

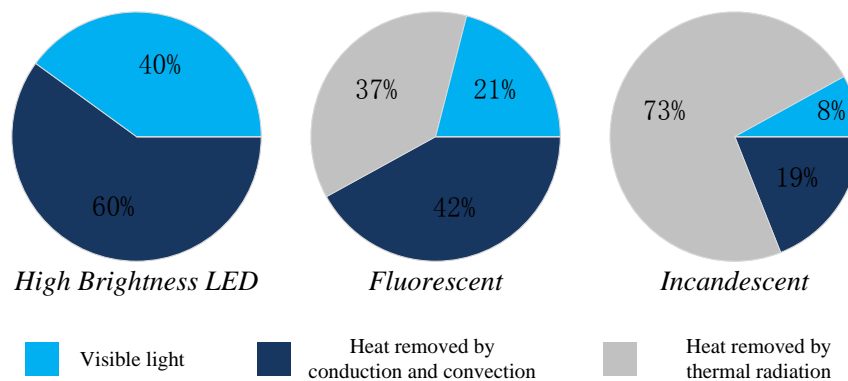


Fig. 7. Power distribution comparison between a HB LED, fluorescent lamp, and an incandescent lamp [10].

The phosphor layer and the lamp cover layer are found to have fairly constant conversion efficiencies for different junction temperatures (i.e., at different  $P_d$ ), and their efficiencies are higher than that of the blue LED layer, especially when junction temperature goes higher. In the experiment, it is found that the phosphor has an efficiency of around 75% and the lamp cover has an efficiency of around 89%. The efficiency of a low-power LED ballast is usually higher than 85%.

According to Fig. 6, it is evident that more efforts should be focused on the conversion efficiency of the blue LED layer (Stage 2), and that there is more room for improvement for this stage than for the others. As LED efficiencies are expected to improve continuously, the power audit information provided here can be used to predict the impact of improved LEDs on the near-future total system efficiency. Finally, the proposed five-stages model and energy flow chart could be extended as a generic model, such that other types of LED-based light sources can be evaluated.

#### IV. IMPACTS OF AMBIENT TEMPERATURE ON THE COMPACT RETROFIT LED BULB

Unlike incandescent lamps in which most of the heat energy from the filament are dissipated to the ambient in the form of infrared radiation (*IR*), the heat energy within an LED can only be dissipated through thermal conduction and convection, that is, from the active area (the LED *P-N* junction) to the underlying printed circuit board, then to the cooling system (such as heatsink), the housing, and finally to the ambient. Fig. 7 gives a comparison of the power distribution among the three most common types of light sources for general illumination, that is, a HB LED, a fluorescent lamp, and an incandescent lamp [10]. Although the LED lamp gives the highest wall-plug efficiency (40% of  $P_d$ ) among the three, it has the most critical burden on thermal design in terms of conduction and convection (60% of  $P_d$ ). If the thermal design is poor, the heat energy will accumulate and heat up the *P-N* junction temperature of the LED, which will subsequently degrade the LED performance in terms

of (1) its lifetime; (2) its color property; (3) its light efficacy; and (4) the reliability of the overall LED system.

It has been reported in [11] that the wall-plug efficiency (the optical power  $P_{opt}$  of an LED chip divided by its input electrical power  $P_d$ ) is typically within the range of 5%-40%. In a practical LED system, if the conversion efficiencies in all stages are considered, including the LED ballast, blue LED, phosphor layer, and lenses, the actual optical output power is even lesser. This implies that with more heat energy, the thermal design will become even more challenging. In Section III, it is illustrated that around 21% of the total energy has been converted as the light output, whereas the rest 79% ends up as heat, in contrast with the value of 60% as shown in Fig.7.

The undesired effects of various heat sources are general to all LED systems. In this section, the impacts of heat sources on a compact retrofit system, which is limited by the same form factor restrictions as existing light bulbs, are examined. Firstly, with a small form factor, the LED ballast must be able to fit with a small fixture. Compact ballasts usually have poor power conversion efficiency as compared with ballasts of a larger size, since their components have to perform multiple tasks (e.g. achieving power factor correction, output current regulation, and dimming, all at the same time) to save space. However, it is difficult to optimize the performance for all tasks simultaneously, and significant heat loss would be generated. Secondly, with the cooling system (heatsink) also restricted to a small size, temperature within the bulb could be high. These form factor constraints do restrict the optimal performance and design of the LED bulb.

Since the LED bulbs can be placed in different lighting fixtures which may not have good ventilation, the study of the effects of the ambient temperature on the luminous performance is important. In order to test the LED bulb at different ambient temperature while its luminous output can still be measured inside the integrating sphere, a methodology has been devised to emulate the ambient change. An extra heating resistor is mounted on heatsink (Fig.4(d)) of the LED bulb so that resistive power dissipation can be controlled to vary the heatsink temperature. Fig.8(a) shows the equivalent

thermal circuit of the setup. The terms  $k_h P_d$  and  $P_R$  represent the heat dissipation of the LED device and the heating resistor, respectively. The junction temperature of the LED can be represented as:

$$T_j = k_h P_d R_{jc} + (k_h P_d + P_R) R_{hs} + T_a \quad (12)$$

Re-arranging (12) gives:

$$T_j = k_h P_d (R_{jc} + R_{hs}) + P_R R_{hs} + T_a \quad (13)$$

By putting the emulated ambient temperature  $T_{a\_emulated}$  as:

$$T_{a\_emulated} = P_R R_{hs} + T_a \quad (14)$$

equation (13) becomes:

$$T_j = k_h P_d (R_{jc} + R_{hs}) + T_{a\_emulated} \quad (15)$$

The equivalent thermal circuit can now be represented as that shown in Fig. 8(b). Therefore, by manually controlling the power dissipation in the heating resistor, the equivalent ambient temperature can be altered and the LED bulb can be tested inside the integrating sphere at different emulated ambient temperature.

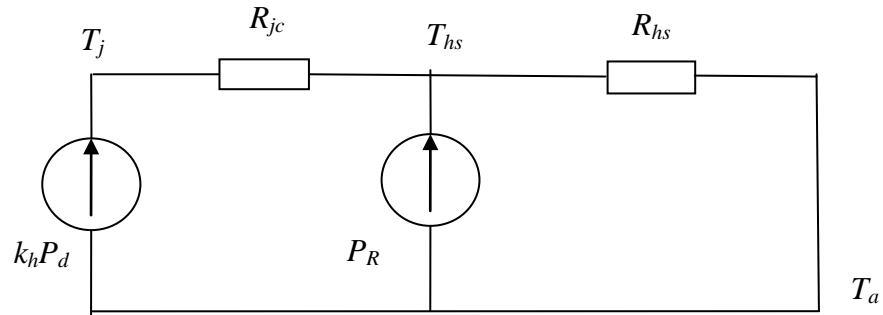


Fig. 8(a) Equivalent thermal circuit including the heat sources of the LED chip and the extra heating resistor.

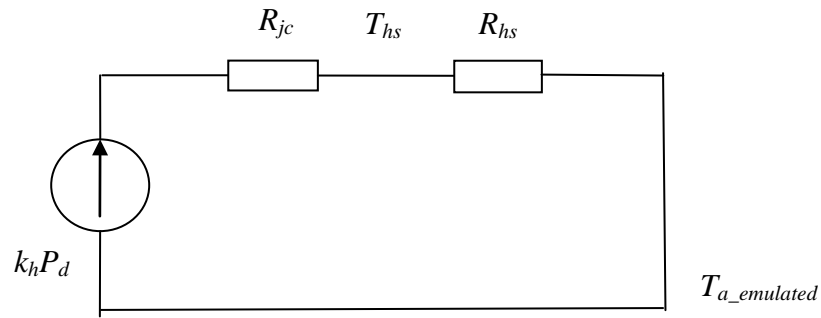


Fig. 8(b) Equivalent thermal circuit of Fig.8 (a) with ambient temperature replaced by emulated ambient temperature

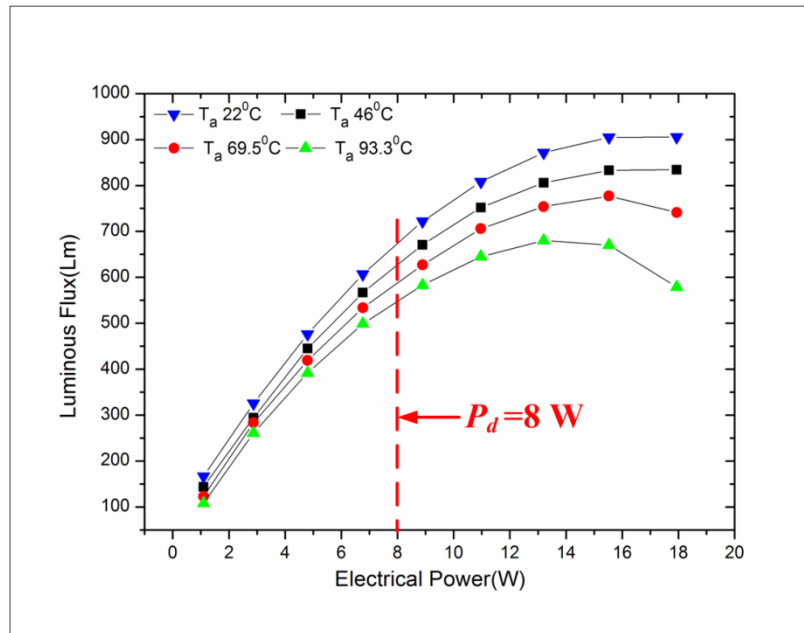


Fig. 9. Measured luminous flux with the LED bulb in the downward position.

Based on this methodology, the LED bulb is tested at different equivalent ambient temperature. In the tests, the LED bulb is placed with the lens (i.e. translucent cover) of the bulb pointing downward. Measurements are made after the LED bulb has been operated for 40 minutes. The luminous flux is measured at different emulated ambient temperature over a range of electrical power. Fig.9 displays four sets of luminous flux measurements at ambient temperature of  $22^\circ\text{C}$ ,  $46^\circ\text{C}$ ,  $69.5^\circ\text{C}$  and  $93.3^\circ\text{C}$ . At the rated power of 8W for the LED device, the luminous flux varies from about 675 lumen at an ambient temperature of  $22^\circ\text{C}$  to 550 lumen at  $93.3^\circ\text{C}$ . For the same temperature range, the luminous efficacy changes from 84 lumen/Watt to 69 lumen/Watt.

Fig.10 shows the measured correlated color temperature (CCT) of the LEB bulb. It is noted that the CCT varies with the ambient temperature. The change of the ambient temperature will alter the junction temperature, which affects the CCT. According to the ANSI C78.377 [15], a nominal CCT of 3000 K should be within  $3045 \pm 175$  K (i.e. within the range from 2870 K to 3220 K). From Fig.10, the measured CCT is within such range from 1W to the rated power of 8W. The measured color rendering index (CRI) is recorded in Fig.11. The CRI variation is found to be very small and within the range of  $81.75^\circ\text{C}$  to  $83^\circ\text{C}$ .

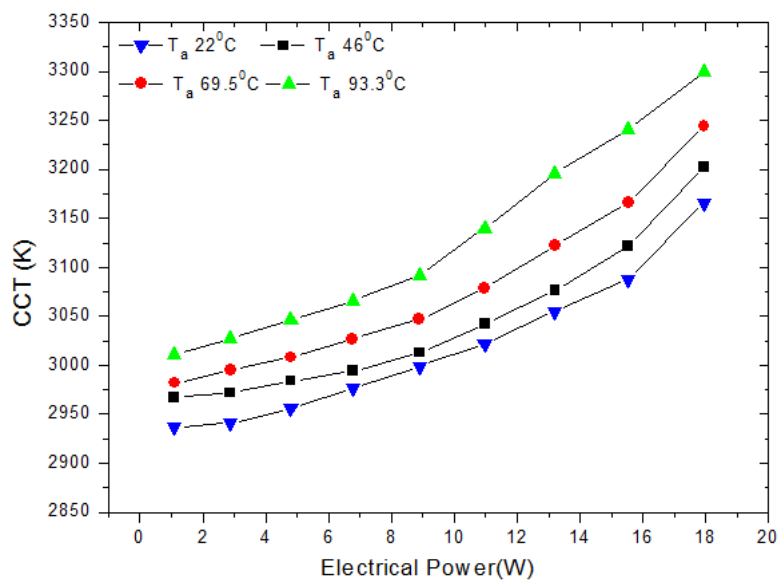


Fig.10 Measured correlated color temperature (CCT) with the LED bulb in the downward position

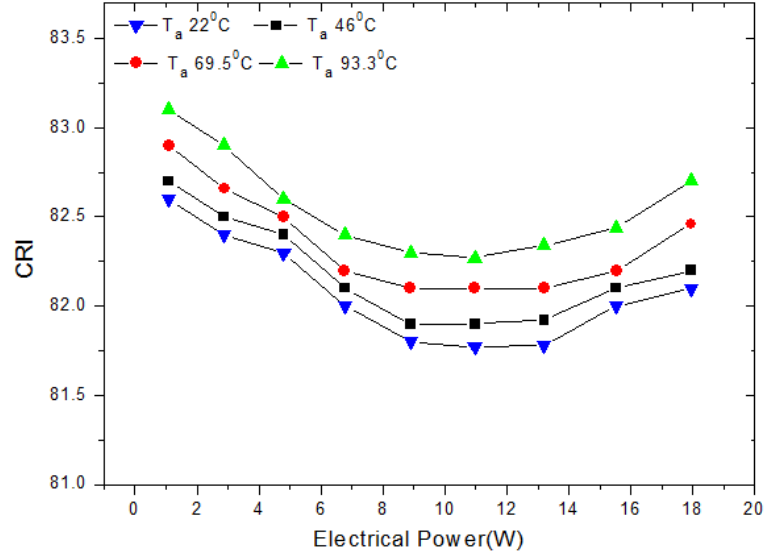


Fig.11 Measured color rendering index (CRI) with the LED bulb in the downward position

The measurements in Fig.9 to Fig.11 show that the luminous flux of the LED bulb is much more sensitive to ambient temperature change than the CCT and CRI. The parabolic shape of the flux-power curves recorded in Fig.9 has been explained by the PET theory [3], which predicts that the peak of the luminous flux curve occurs at the power  $P_d^*$ :

$$P_d^* = -\frac{1 + k_e(T_a - T_o)}{2k_e k_h (R_{jc} + NR_{hs})} \quad \text{for } P_d^* > 0 \text{ W} \quad (12)$$

where  $k_e$  is the coefficient of the rate of change of the luminous efficacy with junction temperature,  $T_o$  is typically set at 25°C in LED data sheet and  $N$  is the number of LED mounted on the heatsink. In this case,  $N=1$  because only one LED device is tested in this experiment. Because the luminous efficacy decreases with increasing junction temperature,  $k_e$  is a negative coefficient. Therefore, the negative denominator of (12) and the minus sign indicate that the overall term in (12) is positive. For the retrofit LED bulb with compact heatsink,  $R_{hs}$  is fixed. According to (12),  $P_d^*$  increases as  $T_a$  increases. This theoretical prediction agrees with the practical measurements shown in Fig.9. For the small heatsink of Fig.4(d), the thermal resistance  $R_{hs}$  is 6.5°C/W. Such a large  $R_{hs}$  is typical and is a major design



constraint for compact LED systems. In order to maximize the luminous flux, LED device with small  $R_{jc}$  and  $k_h$  should be chosen.

For the E27 retrofit LED bulb structure, it is interesting to note that  $P_d^*$  locates beyond the rated power of 8W in Fig.9. If dimming is required, the operating point will fall within the relatively linear part of the parabolic flux-power curves. The initial linear portion of the curves have good efficacy due to low junction temperature. This portion can be used for PWM dimming or  $n$ -level PWM dimming [12], since the light output by these two methods is similar to amplitude dimming due to the linear properties. Energy Star program suggests a continuous dimming range of 35%-100% for dimmable LED products [13]. The flux-power curves of Fig.9 indicate that the E27 retrofit LED bulb can meet such requirement over a wide ambient temperature range.

Tests are also conducted with the LED lens pointing upward. In such position, heat generated by various functional stages will be trapped inside the bulb cover, resulting in an increase in junction temperature of the LED chip. The luminous flux, CCT and CRI measurements have been recorded and compared with the corresponding results obtained with the LED lens pointing downward. Fig.12 shows that the luminous flux will be reduced in the upward position. This is expected because the rise in the junction temperature will reduce luminous efficacy and therefore the luminous flux. However, the junction temperature rise does not significantly affect the CCT and CRI. It is noted in Fig.13 that the CCT will slightly increase, but such increase is within 10 K, which is too small to be noticed by human eyes. Fig.13 indicates that the difference in CRI for the upward and downward positions is also small. Therefore, the orientation of the compact LED bulb affects its luminous flux more than its CCT and CRI from a user's point of view.

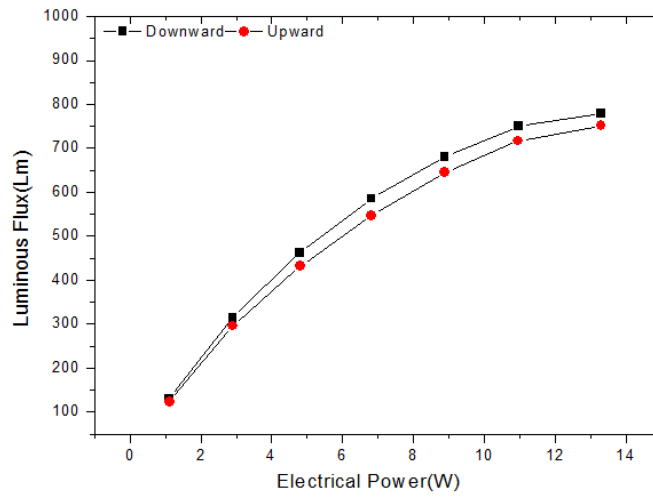


Fig.12 Measured luminous flux

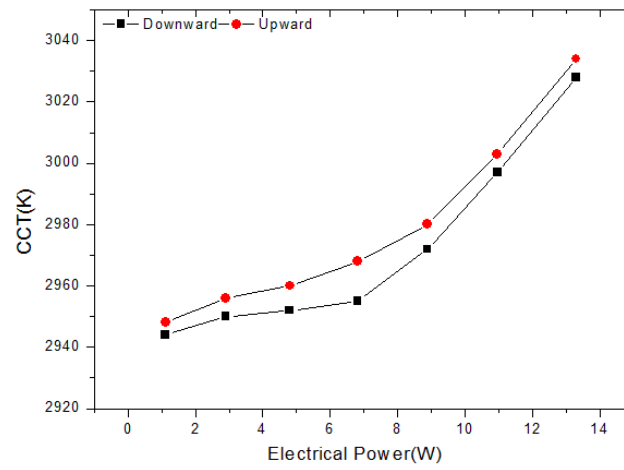


Fig.13 Measured correlated color temperature (CCT)

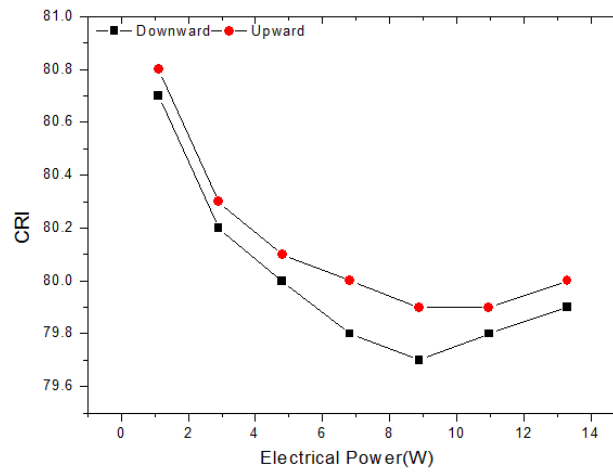


Fig.14 Measured color rendering index (CRI)

## V. CONCLUSIONS

Critical design issues of a compact LED light bulb are addressed. A power flow analysis has been conducted on an E27 retrofit LED bulb to quantify the energy efficiencies of several functional stages, including the blue LED, the phosphor layer and the lenses/lamp cover layer. The power audit shows that the blue LED stage has the lowest energy efficiency, even though blue LED is more efficient than red and green LEDs. The power audit analysis provides information for researchers and design engineers to investigate the scope of efficiency improvement can be targeted in each functional stage. The thermal effects due to the constraint of the small heatsink in compact LED system affect the luminous flux more than the CCT and CRI. Experimental results indicate that the luminous flux is much more sensitive to ambient temperature change, while the CCT and CRI variations with temperature are relatively small. In order to improve the luminous performance, LED devices with small  $k_h$  and  $R_{jc}$ , and phosphor coating and lens with high conversion efficiency should be chosen. Although the power audit does not include the driver circuit, it is envisaged that LED driver without using electrolytic capacitor should be designed in order to prolong the lifetime of the driver in a compact design with stringent constraint on the cooling mechanism.

## ACKNOWLEDGMENT

This work is supported by the Research Grant Council of Hong Kong under the Theme-Based Research Scheme (TBRs) T22-715/12N.

## REFERENCES

- [1] L. Gu, X. Ruan, M. Xu, and K. Yao, "Means of Eliminating Electrolytic Capacitor in AC/DC Power Supplies for LED Lightings," *IEEE Transactions on Power Electronics*, vol. 24, no. 5, May 2009, pp. 1399–1408.
- [2] E. Schubert, T. Gessmann, and J. Kim, *Light emitting diodes*, 2nd ed. Cambridge, U.K.: Cambridge Univ. Press, 2005.
- [3] S. Y. (Ron) Hui and Y. X. Qin, "A General Photo-Electro-Thermal Theory for Light Emitting Diode (LED) Systems," *IEEE Transactions on Power Electronics*, vol. 24, no. 8, Aug. 2009, pp. 1967–1976.
- [4] S. Uddin, H. Shareef, A. Mohamed, M. A. Hannan, and K. Mohamed, "LEDs as energy efficient lighting systems: A detail review," in *2011 IEEE Student Conference on Research and Development*, 2011, pp. 468–472.
- [5] J. Legendziewicz, J. Hanuza, O. Malta, W. Strek, M. Kučera, P. Hasa, and J. Hakenová, "Optical and magneto-optical properties of Ce:YAG," *J. Alloys Compd.*, vol. 451, no. 1, 2008, pp. 146–148.
- [6] C.-Y. Liu, S. W. R. Lee, M. W. Shin, Y.-S. Lai, H.-K. Fu, C.-W. Lin, T.-T. Chen, C.-L. Chen, P.-T. Chou, and C.-J. Sun, "Investigation of dynamic color deviation mechanisms of high power light-emitting diode," *Microelectron. Reliab.*, vol. 52, no. 5, 2012, pp. 866–871.
- [7] S. Wang, X. Ruan, K. Yao, and Z. Ye, "A flicker-free electrolytic capacitor-less ac-dc LED driver," in *2011 IEEE Energy Conversion Congress and Exposition*, 2011, pp. 2318–2325.
- [8] M. R. Krames, O. B. Shchekin, R. Mueller-Mach, G. O. Mueller, L. Zhou, G. Harbers, and M. G. Craford, "Status and Future of High-Power Light-Emitting Diodes for Solid-State Lighting," *J. Disp. Technol.*, vol. 3, no. 2, Jun. 2007, pp. 160–175.
- [9] A.A.Setlur, "phosphor for LED-based solid-state lighting," *Electrochem. Soc. Interface*, 2009, pp. 32–36.

- [10] O. Lighting, "Power conversion." [Online]. Available: <http://www.omslighting.com/ledacademy/574/>.
- [11] "Fact or Fiction – LEDs don't produce heat," *LEDs Magazine*, 2005. [Online]. Available: <http://ledsmagazine.com/features/2/5/8>.
- [12] S. C. Tan, "General  $n$ -level driving approach for improving electrical-to-optical energy-conversion efficiency of fast-response saturable lighting devices," *IEEE Transactions on Industrial Electronics*, vol. 57, no. 4, Apr. 2010, pp. 1342–1353.
- [13] "Energy Star Program Requirements Product Specifications for Luminaires (Lighting Fixtures) Version 1.0." 2011.
- [14] S. Li, H.T. Chen, S.C. Tan, E. Waffenschmidt and S.Y.R. Hui, "Critical design issues of retrofit Light-Emitting Diode Light Bulb", *IEEE Applied Power Electronics Conference (APEC)*, Fort Worth, Texas, 16-20 March, 2014, pp:531-536.
- [15] American National Standard, Specifications for Chromaticity of Solid State Lighting Products, ANSI C78.377 (American National Standards Institute, 2008).